

Preparation and Characterization of Multiferroic BiFeO₃ Films

H.Naganuma, A.Kovacs*, Y.Hirotsu*, Y.Inoue, and S.Okamura

Department Applied Physics, Tokyo University of Science, 1-3 Kagurazaka, Shinjuku-ku, Tokyo 162-8601, Japan

Fax: 81-3-3260-4272 (Ext. 2442), e-mail: naganuma@rs.kagu.tus.ac.jp

* ISIR, Osaka University, 8-1 Mihogaoka, Ibaraki, Osaka 567-0047, Japan

Fax: 81-6-6879-8431, e-mail: andras22@sanken.osaka-u.ac.jp

Transmission electron microscopy (TEM) observation was used to study a polycrystalline BiFeO₃ film fabricated by a chemical solution deposition (CSD) on Pt/Ti/SiO₂/Si(100) substrates. Cross-sectional TEM images and corresponding selected area diffraction patterns (SAED) as well as x-ray diffraction (XRD) patterns indicated that the polycrystalline single phase of the BiFeO₃ film was formed after annealing at 823 K for 10 min. Interfacial structural analysis making use of a high resolution cross-sectional TEM observation showed that a 1~2-nm-thick amorphous layer was formed only at the interface of the bottom electrode, and we found this amorphous layer deteriorates the leakage current quality. Ferroelectric hysteresis loops were measured by using a high frequency of 100 kHz system in order to suppress the leakage current component. The remanent polarization and the electrical coercive field of the BiFeO₃ film were around 46 $\mu\text{C}/\text{cm}^2$ and 230 kV/cm, respectively at room temperature. At 10 K, the remanent magnetization and a magnetic coercivity were around 2 emu/cm³ and 0.5 kOe, respectively. However each parameter disappears at least 40 K. A broad peak was observed at 70 K in zero-field-cooling curve, which indicates a spin glass behavior of the BiFeO₃ film.

Key words: BiFeO₃ films, Transmission electron microscopy, Multiferroics, Magnetism

1. INTRODUCTION

Multiferroic materials couple electric, magnetic, and structural order parameters, which results in a simultaneous appearance of ferroelectricity, ferromagnetism, and ferroelasticity. Therefore, multiferroic materials have attracted much interest as a candidate for a future multi-valued memory device. However a number of multiferroic materials have their ferro-character only at low temperature.^{1, 2)} BiFeO₃ is one of a few materials which combine a ferroelectricity and a parasitic magnetism above the room temperature,^{3, 4)} therefore recently BiFeO₃ has been intensively studied.⁵⁾ In the previous study,⁶⁾ we fabricated the polycrystalline BiFeO₃ films by a chemical solution deposition (CSD) followed by a post-annealing at 823 K for 10 min in air, and investigated the ferroelectricity as well as the ferromagnetism. In the report, a zero-field-cooling curve showed the broad peak at low temperature, which indicates the presence of superparamagnetism, spin freezing or cluster glasses. The superparamagnetic nanoparticles are too small to be analyzed by a conventional X-ray diffraction (XRD) which we used in the previous study, therefore the cause of the broad peak in the zero-field-cooling curve is unclear. In present study, we investigate the fine structure of the BiFeO₃ film by using a transmission electron microscopy (TEM) in order to understand the origin of the broad peak in the zero-field-cooling curve. We also discuss the ferroelectricity and the ferromagnetism of the BiFeO₃ film using a

high-frequency ferroelectric measurement system and a superconducting quantum interface device (SQUID) magnetometer.

2. EXPERIMENTAL PROCEDURE

BiFeO₃ films were fabricated by a CSD on Pt/Ti/SiO₂/Si(100) substrates. A post-deposition annealing was performed by a rapid thermal annealing in the range from 723 to 1073 K for 10 min in air. Upper and bottom Pt electrodes were deposited by an rf magnetron sputtering. The film thicknesses were around 200-300 nm. The film structure was investigated by using a TEM (JEOL 3000F) as well as a conventional $\theta/2\theta$ XRD. Ferroelectric hysteresis loops were measured by making use of the high frequency of 100 kHz system produced by TOYO Corporation (FCE-1A type ferroelectric test system). Leakage current density was measured by HP 4140B. Driving voltage was applied to the bottom electrode. The magnetic properties were measured by the SQUID (MPMS-XL) magnetometer with a magnetic field of up to 50 kOe.

3. RESULTS

3.1 XRD analysis

Figure 1 shows the XRD patterns for the BiFeO₃ films as a function of annealing temperature. Dashed lines indicate the peak positions of BiFeO₃ structure. Below 923 K, many diffraction peaks corresponding to the BiFeO₃ structure were observed, and no other secondary phases could be observed, indicating the formation

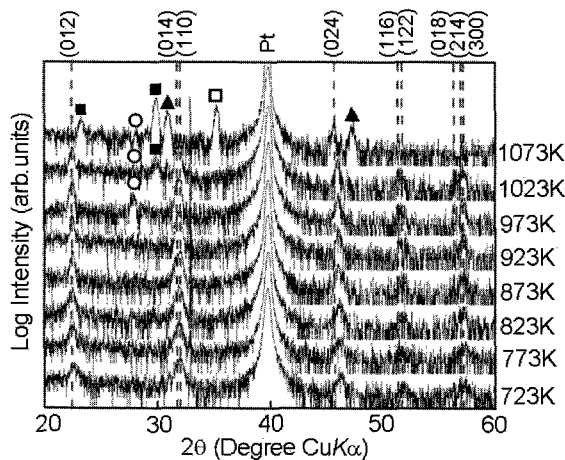


Figure 1 X-ray diffraction patterns for BiFeO₃ films as a function of annealing temperature. ○: Bi₂O₃, ■: Bi₂Pt, □: Fe₂O₃, ▲: unknown.

of the polycrystalline BiFeO₃ films. Additional peaks of Bi₂O₃, Bi₂Pt and Fe₂O₃ phases as well as unknown peaks were observed above 973 K. Next, we measured the magnetic and the ferroelectric properties of the polycrystalline BiFeO₃ film annealed at 823 K for 10 min.

3.2 Magnetic and ferroelectric properties

Figure 2(a) shows ferroelectric hysteresis loop, 2(b) shows the leakage current density-electric field characteristics, 2(c) and 2(d) show the magnetization curves measured at 10K and 40 K, respectively for the BiFeO₃ film annealed at 823 K for 10 min. Ferroelectric hysteresis loops of unsaturated lose-shape were observed at the frequency below 2 kHz (not shown here). However when we increased the measurement frequency up to 100 kHz, a ferroelectric hysteresis loop of well-saturated shape with the relatively high remanent polarization of 46 $\mu\text{C}/\text{cm}^2$ and the electric coercivity field of 230 kV/cm

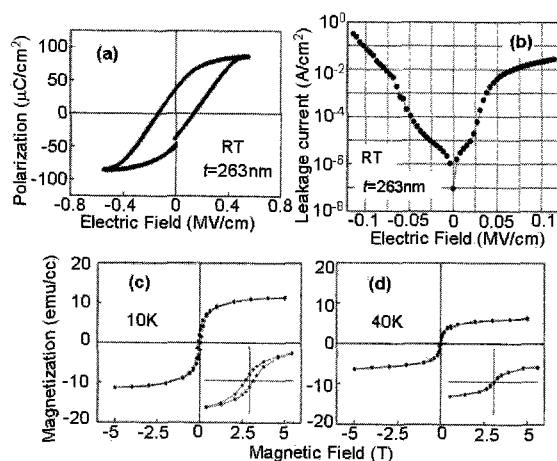


Figure 2 Ferroelectric hysteresis loop (a), leakage current density-electric field characteristics (b), magnetization curves measured at 10K (c) and 40 K (d), respectively for BiFeO₃ film annealed at 823 K for 10 min.

was obtained as shown in Fig 2(a). These parameters of the polycrystalline BiFeO₃ film are comparable to the polycrystalline PZT film.⁷⁾ The leakage current density was 10^{-2} A/cm² order at 0.1 MV/cm, which indicates the high leakage current density of the BiFeO₃ film [Fig. 2(b)]. Therefore, it could be considered that the unsaturated lose shape of the ferroelectric hysteresis loops measured at the low frequency is attributed to the high leakage current density of the BiFeO₃ films. The leakage current density curve showed three kinds of incline angles, indicating the leakage current mechanism is changed as a function of the electric field. The detail of leakage current mechanism is discussed elsewhere.⁶⁾ The increment ratio of the leakage current density in the negative electric field was higher than that of the positive electric field. This reason will be discussed in the next section, 3.3. In Fig 2(c), the saturation magnetization at 10 K of the BiFeO₃ film was 11 emu/cm³. The expanded magnetization curve of the inset showed the coercivity of 0.5 kOe and the remanent magnetization of 2 emu/cm³, respectively, indicating the ferromagnetic order at low temperature. When increasing the measurement temperature to 40 K, the saturation magnetization decreased drastically to 6 emu/cm³, and the coercivity as well as the remanent magnetization disappeared. The magnetic curve measured at 300 K was almost same as that of 40 K. The magnetization curve above 40 K of the BiFeO₃ film seems like a typical behavior of the parasitic magnetic materials. According to our previous study,⁶⁾ the blocking temperature was observed at 70 K in the zero-field cooling curve. Thus, the ferromagnetic order in the BiFeO₃ film disappeared below the blocking temperature. In order to understand the cause of the blocking temperature as well as the asymmetric leakage current, we investigated the structure in detail by the TEM observation.

3.3 Cross-sectional TEM observations

Figure 3 shows a cross-sectional TEM image (a), the high resolution TEM images around the interface of the upper electrode (b) and the bottom electrode (c) of the polycrystalline BiFeO₃ film annealed at 823 K for 10 min. As shown in Fig 3(a), a thin layer with higher brightness was observed at the interface of the bottom electrode side. The high resolution TEM image as shown in Fig. 3(c) revealed that the thin layer is an amorphous structure of the thickness of 1~2 nm, which was continuously formed in the area that we observed. In order to clarify the amorphous composition, we carried out EELS elemental maps of iron and oxygen atoms. However, it was difficult to find any differences by using the EELS elemental mapping. This difficulty is attributed to the very thin amorphous layer. By contrast, no interfacial layer was observed at the upper electrode side as shown in Fig. 3(b). From these results, it could be considered that the asymmetric leakage current density curve as shown in Fig. 2(b) is attributed to the formation of the thin amorphous interfacial layer at the bottom electrode. This amorphous interfacial layer deteriorated the leakage current quality in the BiFeO₃ film. Recently, a few researchers reported⁸⁾ that the grain boundary of the polycrystalline BiFeO₃ film affects the leakage current density, though there are no

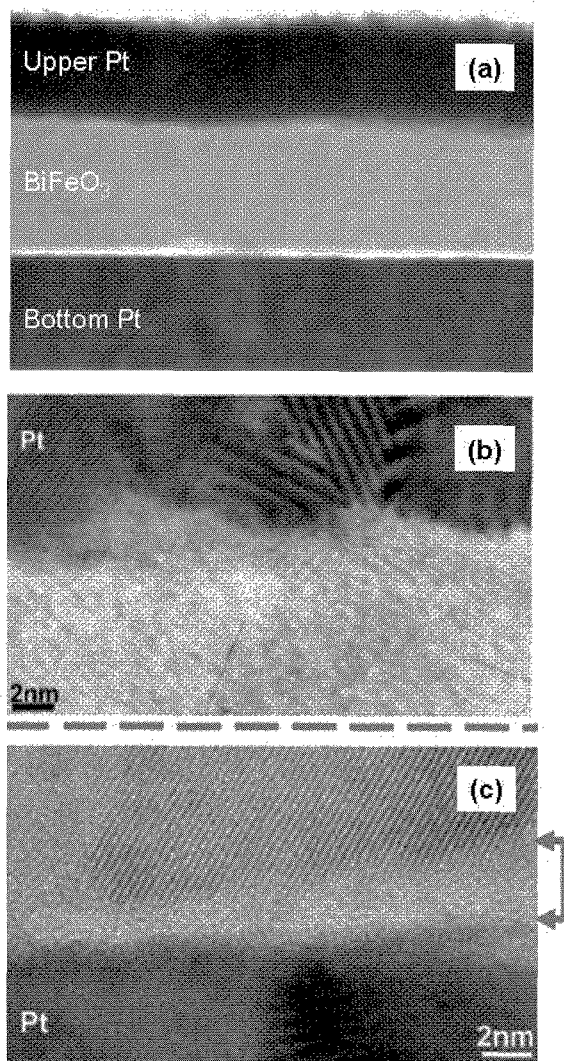


Figure 3 Cross-sectional TEM image (a), high resolution TEM images at around the interface of the upper electrode (b) and bottom electrode (c) for BiFeO₃ film.

reports in term of the structure of the grain boundary in detail of the polycrystalline BiFeO₃ film. Hence, we investigate the grain boundary of the BiFeO₃ film annealed at 823 K for 10 min.

Figure 4 shows the high resolution TEM image at the grain boundary and the selected area diffraction patterns from wide area of the polycrystalline BiFeO₃ film. At the grain boundary, no other secondary phase such as grain boundary phase could be observed. We also observed the many grain boundaries, though the grain boundary phase was not observed in the present polycrystalline BiFeO₃ film. In Fig. 4(d), only the diffraction spots due to the BiFeO₃ structure were observed in the selected area diffraction patterns indicating that the single phase of polycrystalline BiFeO₃ film was formed. The indices of the selected area diffraction patterns were located close to each other, which indicates approximal grains rotated their crystal axis with a small angle.

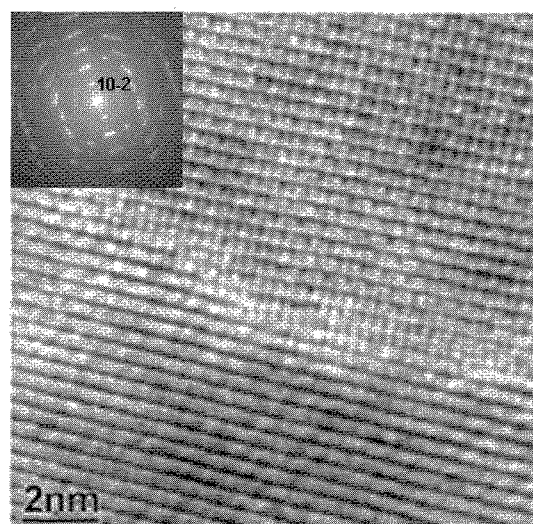


Figure 4 High resolution TEM image at the grain boundary (a), corresponding FFT images (b), (c) and selected area diffraction patterns (d) of polycrystalline BiFeO₃ film.

4. DISCUSSION

As mentioned in the previous paper,⁶⁾ the BiFeO₃ film annealed at 823 K for 10 min showed the blocking temperature at around 70 K. This blocking temperature was not attributed to the magnetic transition temperature of the BiFeO₃ material, because Néel temperature of the BiFeO₃ material is around 653 K.³⁾ In this study, we investigated the structure of the BiFeO₃ film in detail, and we concluded that the present specimen was a single phase of the polycrystalline BiFeO₃ film without any secondary phase including the grain boundary phase, indicating that the observed blocking temperature is not caused by the superparamagnetic nanoparticles. Therefore, it can be considered that the blocking temperature is attributed to a spin glass behavior of BiFeO₃ material. There exist a lot of mechanisms due to the spin glass behavior. For example, in the case of the Fe-Au alloy, small amount of the iron atoms dispersed in the nonmagnetic matrix of gold develop the spin glass phenomenon.⁹⁾ Because of the small amount of the iron atoms as well as the matrix including the iron element in the case of the BiFeO₃, it is difficult to detect the dispersed iron atoms by using the TEM and the EELS elemental maps in this study. Thus, further magnetic measurement is necessary to determine the origin of the spin glass behavior in the present BiFeO₃ film.

In the present study, the ferromagnetic order with the small coercivity and the small remanent magnetization were observed at 10 K, though the ferromagnetic order was disappeared at 40 K. The orthoferrite such as LaFeO₃ and LuFeO₃ of the parasitic magnetic materials shows the ferromagnetism at low temperature due to the magnetic order of rare earth atoms. Bismuth is a diamagnetism element even at low temperature, so that the magnetic order at low temperature in the BiFeO₃ film might be related to the iron atoms.

5. CONCLUSIONS

We have fabricated BiFeO₃ films by the CSD and investigated the structure as well as the multiferroic properties of the magnetism and the ferroelectricity. The high resolution TEM observation showed that the single phase of the polycrystalline BiFeO₃ film was formed after annealed at 823 K for 10 min without any secondary phase such as a grain boundary phase or superparamagnetic nanoparticle. Thus, it could be considered that the blocking temperature at 70 K in the zero-field-cooling is attributed to the spin glass behavior of the BiFeO₃ film. An interfacial structural analysis making use of the cross-sectional TEM observation revealed that the asymmetric leakage current curve is attributed to the formation of the amorphous thin layer at the interface of the bottom electrode. The remanent magnetization and the magnetic coercivity were 2 emu/cm³ and 0.5 kOe, respectively at 10 K, though both parameters disappeared at 40 K. The remanent polarization and the electric coercivity field were 46 μC/cm² and 230 kV/cm, respectively at room temperature. These ferroelectric properties are comparable to those of the polycrystalline PZT films.

ACKNOWLEDGMENTS

This study was partly supported by the Grand-in-Aid for Young Scientist Startup Program (Grant No. 18860070) from the Ministry of Education, Culture, Sports, Science and Technology, Japan. The authors wish to express gratitude to Hironobu Matsumoto of TOYO Corporation for ferroelectric measurement using FCE-1A type ferroelectric system. The authors also wish to acknowledge the measurements of EELS mapping using the LEO-922 TEM by the Dr. Hirata of ISIR, Osaka University.

REFERENCES

- [1] Dae Ho Kim, Ho Nyung Lee, Maria Varela, and Hans M. Christen, *Appl. Phys. Lett.*, **89**, 162904 (2006).
- [2] Z. H. Chi, C. J. Xiao, S. M. Feng, F. Y. Li, C. Q. Jin, X. H. Wang, R. Z. Chen, and L. T. Li, *J. Appl. Phys.*, **98**, 103519 (2005).
- [3] S. V. Kiselev, R. P. Ozerov, and G. S. Zhdanov, *Sov. Phys.* **7**, 742 (1963).
- [4] Yu. N. Venevtsev, G. Zhdanow, and S. Solov'ev, *Sov. Phys. Crystallogr.*, **4**, 538 (1960).
- [5] for example, T. Zhao, A. Scholl, F. Zavaliche, K. Lee, M. Barry, A. Doran, M. P. Cruz, Y. H. Chu, C. Ederer, N. A. Spaldin, R. R. Das, D. M. Kim, S. H. Baek, C. B. Eom and R. Ramesh, *Nature materials*, **5**, 823 (2006).
- [6] H. Naganuma and S. Okamura, *J. Appl. Phys.* (2007). *in press*
- [7] H. Shima, H. Naganuma, and S. Okamura, *Jap. J. Appl. Phys.* **45**, 7279 (2006).
- [8] C. F. Chung, J. P. Lin and J. M. Wu, *Applied Physics Letters*, **88**, 242909 (2006).
- [9] V. Cannella and J. A. Mydosh, *Phys. Rev.* **B6**, 4220 (1972).

(Received December 28, 2006; Accepted December 28, 2006)